

Motion as a Causal Mediator in Studies of Functional Connectivity Alterations in Children with Autism Spectrum Disorder

Jialu Ran¹, Sarah Shultz², Benjamin Risk¹ and David Benkeser¹

¹*Department of Biostatistics and Bioinformatics, ²Department of Pediatrics, Emory University*

github.com/thebrisiklab



Collaborators

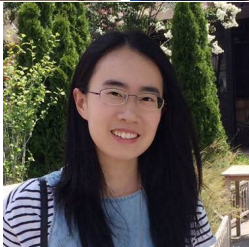


Figure: Jialu Ran, Sarah Shultz, David Benkeser, Xiyan Tan, Zihang Wang

Introduction: Autism spectrum disorder

Autism spectrum disorder (ASD):

- Approximately 1 in 36 children in the US (Maenner 2023).
- Deficits in social communication and interaction; restricted and repetitive behaviors, interests, and activities.
- Functional connectivity is used to study ASD.
- Correlations between regions:

$$\text{Functional connectivity}_{ij} = \text{Corr}(Y_{i,\text{seed},t}, Y_{i,j,t}) = Y_{ij}.$$

- In ASD, disruptions of functional connectivity thought to involve the default mode network (Yerys et al. 2015).

Default mode decreased connectivity

The intrinsic brain architecture in autism A Di Martino *et al.*

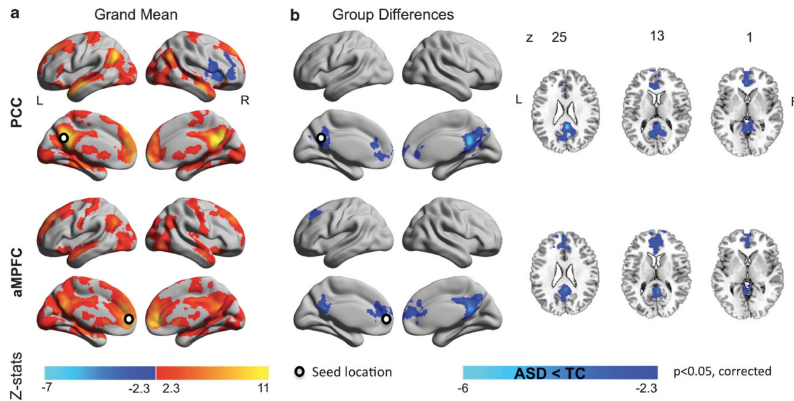


Figure: Di Martino et al. (2014)

Introduction: Movement during scan

Problem: Motion

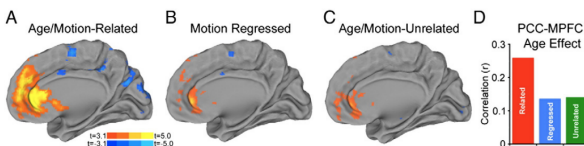
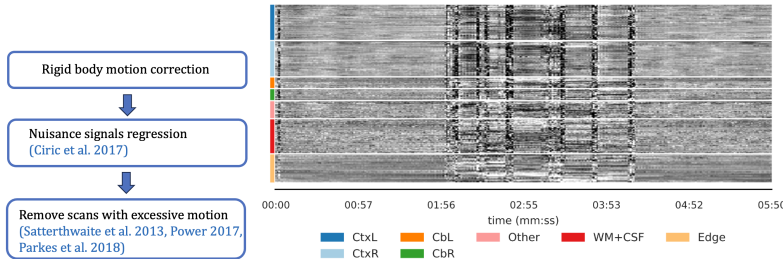


Fig. 6. Effect of motion on estimates of age-related connectivity change from a posterior cingulate seed. In a sample of 421 subjects where age and motion were related, increasing subject age was associated with increased connectivity between the PCC and the MPFC (A). This effect, while still significantly present, was attenuated when motion was included as a confound regressor in the group level analysis (B) or when the *age/motion-unrelated* subsample of 348 subjects was used (C). The correlation of age with pairwise PCC-MPFC connectivity was reduced substantially when motion was taken into account (D).

- Satterthwaite et al. (2012): age-related differences partly due to younger children moving more than older children.

Problem I: Motion Artifacts



- Existing motion control using regression is inadequate because motion patterns are complex (Power et al. 2014).
- Current best practices **remove scans with excessive motion**.
- The prevailing view in neuroimaging statistics is that motion artifacts mask the underlying neural signals of interest.

Problem II: Motion QC creates selection bias

- Motion control leads to drastic reductions in sample size.
- ABCD study **removed 60 – 75%** of children due to excessive motion (Marek et al. 2022, Nielsen et al. 2019).
- This creates selection bias, disproportionately selecting for: higher SES, White participants, older, females, higher neurocognitive skills, fewer neurodevelopmental problems (Cosgrove et al. 2022).
- Unethical?

Previous work: selection bias

M.B. Nebel, D.E. Lidstone, L. Wang et al.

NeuroImage 257 (2022) 119296

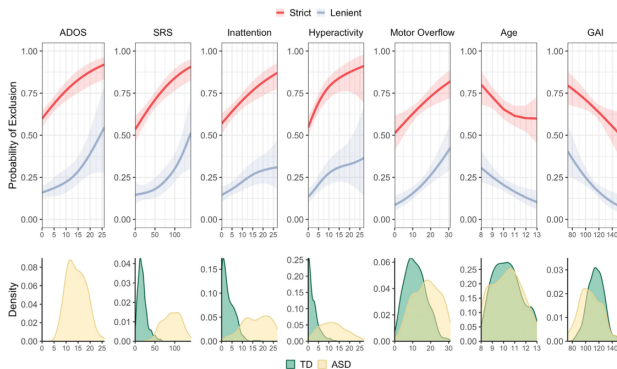
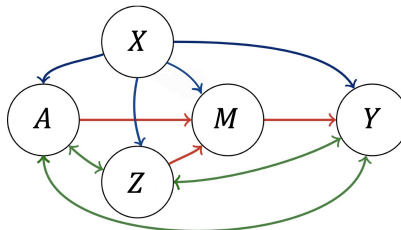


Fig. 4. rs-fMRI exclusion probability changes with phenotype and age. Univariate analysis of rs-fMRI exclusion probability as a function of participant characteristics. From left to right: Autism Diagnostic Observation Schedule (ADOS) total scores, social responsiveness scale (SRS) scores, inattentive symptoms, hyperactive/impulsive symptoms, total motor overflow, age, and general ability index (GAI) using the lenient (slate blue lines, all FDR-adjusted $p < 0.01$), and strict (red lines) motion quality control (all FDR-adjusted $p < 0.03$). Variable distributions for each diagnosis group (included and excluded scans) are displayed across the bottom panel (TD=typically developing, green; ASD=autism spectrum disorder, yellow).

Causal mediation approach: a controversial graph

Our approach treats motion as a mediator:



- $Y \in \mathbb{R}$: functional connectivity between two locations in the brain
- $A \in \{0, 1\}$: non-ASD (0), ASD (1)
- $M \in \mathbb{R}$: a motion variable (mean framewise displacement)
- X : demographic confounders (age, sex and handedness)
- Z : variables related to autism symptomatology (autism diagnostic score, IQ, medication status)

Motion as a Causal Mediator in Studies of Functional Connectivity Alterations in Children with Autism Spectrum Disorder

Nonparametric Motion Control in Functional Connectivity Studies in Children with Autism Spectrum Disorder

Jialu Ran¹, Sarah Shultz², Benjamin Risk¹ and David Benkeser¹

¹*Department of Biostatistics and Bioinformatics, ²Department of Pediatrics, Emory University*

github.com/thebrisklab

Standard approach with linear regression

Consider the linear regression model currently used in neuroimaging studies (Di Martino et al. 2014):

$$Y_i = \beta_0 + \beta_1 A_i + \beta_2 M_i + \sum_{k=3}^p \beta_k X_{ik} + \epsilon_i, \quad i \in \{i : \Delta_i = 1\} .$$

- Linear model for motion effect is not sufficient (Power et al. 2014).
- Removes a lot of data (selection bias).

Initially, consider non-parametric model:

$$Y_i = \mu_{Y|A,M,X}(A_i, M_i, X_i) + \epsilon_i ,$$

where $\mu_{Y|A,M,X}$ is an arbitrary function of (A, M, X) .

- The effect of A_i is no longer straightforward:

$$\mu_{Y|A,M,X}(1, m, x) - \mu_{Y|A,M,X}(0, m, x)$$

is a multivariate function of m and x , hard to interpret.

- Non-parametric inference is challenging and slow, not \sqrt{n}

Marginal effects

This motivates us to consider marginal effects:

$$\int \{\mu_{Y|A,M,X}(1, m, x) - \mu_{Y|A,M,X}(0, m, x)\} p_{M,X}(m, x) dm dx$$

This standardizes motion to the same level in both groups.

- But includes motion artifacts.
- Neuronal signal may be washed out motion artifacts.

Set motion to zero?

Suppose we set $m = 0$:

$$\int \{\mu_{Y|A,M,X}(1, 0, x) - \mu_{Y|A,M,X}(0, 0, x)\} p_X(x) dx$$

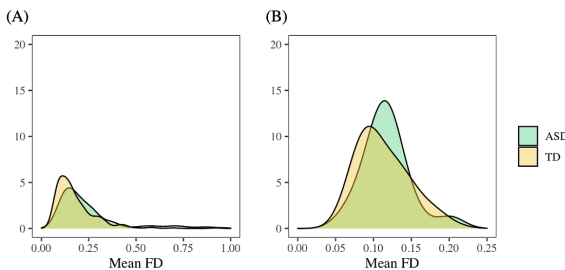
However, we never observe $m = 0$: all children move at least a little bit.

Hence, we can't estimate this non-parametrically.

Stochastic Intervention

Stochastic intervention assigns a motion value based on a random draw from a specified distribution.

For both non-ASD and ASD children, replace motion M by tolerable motion $M_0 \sim P_{M|\Delta=1,0,X}$



Tolerable motion distribution

Instead, we consider marginalizing motion with respect to a given “tolerable motion distribution”:

$$\int \{ \mu_{Y|A,M,X}(1, m, x) - \mu_{Y|A,M,X}(0, m, x) \} p_{M|\Delta=1,A,X}(m|0, x) p_X(x) dm dx. \quad (1)$$

- Issue: ASD is heterogeneous. Children who move less tend to have less severe symptomatology, Z .

ASD symptomatology

We revise our non-parametric model:

$$Y_i = \mu_{Y|A,M,X,Z}(A_i, M_i, X_i, Z_i) + \epsilon_i,$$

and rewrite (1) as

$$\begin{aligned} & \int \left\{ \mu_{Y|A,M,X,Z}(1, m, x, z) p_{Z|A,M,X}(z|1, m, x) \right. \\ & \quad \left. - \mu_{Y|A,M,X,Z}(0, m, x, z) p_{Z|A,M,X}(z|0, m, x) \right\} \\ & p_{M|\Delta=1,A,X}(m|0, x) p_X(x) dz dm dx. \end{aligned}$$

Issue:

- $p_{Z|A,M,X}(z|1, m, x) p_{M|\Delta=1,A,X}(m|0, x)$ results in restricting the ASD symptomatology (because children that move less have less severe autism).

Motion-Controlled Estimand (MoCo)

$$\int \left[\{ \mu_{Y|A,M,X,Z}(1, m, x, z) p_{Z|A,X}(z|1, x) \right. \\ \left. - \mu_{Y|A,M,X,Z}(0, m, x, z) p_{Z|A,X}(z|0, x) \} \right. \\ \left. p_{M|\Delta=1,A,X}(m|0, x) p_X(x) \right] dz dm dx .$$

Assumption (Common support (positivity))

Let $P(B)$ be the probability measure of $\{Y, A, M, X, Z\}$ on some set B . Let $P^*(B)$ be the measure corresponding to the joint density $p_{Y|A,M,X,Z}(y|a, m, x, z) p_{Z|A,X}(z|a, x) p_{M|\Delta=1,A,X}(m|0, x) p_X(x)$.

We assume $P^* \ll P$.

It follows that if $P^*(B) > 0$ then $P(B) > 0$. This ensures that it is possible to observe functional connectivity in the ASD group across combinations of tolerable motion levels and more severe symptomatology.

Estimation: one-step estimator

Plug-in estimator:

$$\theta_{n,a} = \int \mu_{n,Y|a,M,X,Z}(m, x, z) p_{n,Z|a,X}(z | x) p_{n,M|\Delta=1,A,X}(m | 0, x) p_{n,X}(x) dz dm dx$$

Not robust. One-step estimator:

$$\theta_{n,a}^+ = \theta_{n,a} + \frac{1}{n} \sum_{i=1}^n D_{a,P_n}(O_i)$$

- $D_{a,P}(O)$ [EIF] estimated using sequential regressions with Super-Learner and highly adaptive lasso for motion density estimation.
- Asymptotically normal.
- Multiple robustness.

Theorem (Efficient Influence Function)

Define

$$\pi_a(x) = P(A = a | X = x),$$

$$\bar{\pi}_0(x) = P(A = 0 | X = x)P(\Delta = 1 | A = 0, X = x),$$

$$r_a(m, x, z) = \frac{p_{M|\Delta=1,0,X}(m | x)}{p_{M|a,X,Z}(m | x, z)}.$$

In a nonparametric model, the efficient influence function for θ_a evaluated on an observation O_i is

$$\begin{aligned} D_{P,a}(O_i) &= \frac{\mathbb{1}_a(A_i)}{\pi_a(X_i)} r_a(M_i, X_i, Z_i) \{Y_i - \mu_{Y|a,M,X,Z}(M_i, X_i, Z_i)\} \\ &\quad + \frac{\mathbb{1}_a(A_i)}{\pi_a(X_i)} \{\eta_{\mu|a,Z,X}(X_i, Z_i) - \xi_{\eta|a,X}(X_i)\} \\ &\quad + \frac{\mathbb{1}_{a,1}(A_i, \Delta_i)}{\bar{\pi}_0(X_i)} \{\eta_{\mu|a,M,X}(M_i, X_i) - \xi_{\eta|a,X}(X_i)\} + \xi_{\eta|a,X}(X_i) - \theta_a. \end{aligned}$$

\sqrt{n} -Convergence

Theorem (Asymptotic normality)

Under the following assumptions,

- (i) Positivity of estimates: $\pi_{n,a} > \epsilon_1$ for some $\epsilon_1 > 0$, $\bar{\pi}_{n,0} > \epsilon_2$ for some $\epsilon_2 > 0$, and $\frac{p_{n,M|\Delta=1,0,X}}{p_{n,M|a,X,Z}} < \epsilon_3$ for some $\epsilon_3 < \infty$;
- (ii) $n^{1/2}$ -convergence of second order terms...
- (iii) $L^2(P)$ -consistent influence function estimate:

$$\int [\{D_{a,P_\ell}(o) - D_{a,P_n}(o)\}^2] dP(o) = o_P(1),$$

where P_ℓ denotes the limit of P_n as $n \rightarrow \infty$.

- (iv) Donsker influence function estimate: D_{a,P_n} falls in a P -Donsker class with probability tending to 1.

Then,

$$\theta_{n,a}^+ - \theta_a = \frac{1}{n} \sum_{i=1}^n D_{a,P}(O_i) + o_P(n^{-1/2})$$

and

$$n^{1/2}(\theta_{n,a}^+ - \theta_a) \Rightarrow N(0, E[D_{P,a}(O)^2]).$$

Multiple robustness

	$\mu_{n,Y A,M,X,Z}$	$\eta_{n,\mu A,M,X}$	$\xi_{n,a,\eta X}$	$\bar{\pi}_{n,0}$	$\pi_{n,a}$	$p_{n,M \Delta=1,A,X}$	$p_{n,M A,X,Z}$
(B2.1)					✓	✓	✓
(B2.2)			✓			✓	✓
(B2.3)	✓	✓		✓	✓		
(B2.4)	✓				✓	✓	
(B2.5)	✓		✓			✓	

Table: Theorem: multiple robustness. Each row indicates a setting for consistency, where check marks indicate the nuisance parameters which, when they converge to true functions, then $E[D_{P',a}(O)] = 0$, and $\theta_{n,a}^+ \rightarrow \theta_a$.

Simultaneous confidence bands

So far, we've been working with a single region. Extend to multiple regions:

$$\begin{pmatrix} \theta_{n,1,1}^+ - \theta_{n,0,1}^+ \\ \vdots \\ \theta_{n,1,J}^+ - \theta_{n,0,J}^+ \end{pmatrix} - \begin{pmatrix} \theta_{1,1} - \theta_{0,1} \\ \vdots \\ \theta_{1,J} - \theta_{0,J} \end{pmatrix} \rightarrow N \left\{ \begin{pmatrix} 0 \\ \vdots \\ 0 \end{pmatrix}, \text{Cov} \begin{pmatrix} D_{1,P,1}(O) - D_{0,P,1}(O) \\ \vdots \\ D_{1,P,J}(O) - D_{0,P,J}(O) \end{pmatrix} \right\}$$

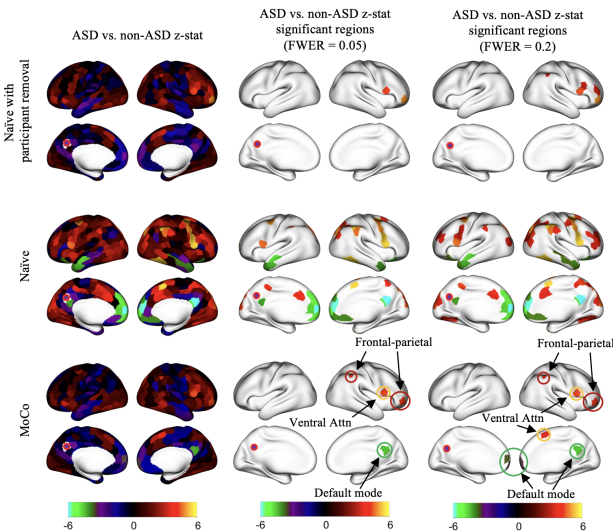
- Calculating simultaneous confidence bands from the influence function is straightforward.
- For $\mathbf{O}_i \in \mathbb{R}^J$, calculate sample correlation matrix using $[D_{1,P,1}(\mathbf{O}_1) - D_{0,P,1}(\mathbf{O}_1)], \dots, [D_{1,P,J}(\mathbf{O}_n) - D_{0,P,J}(\mathbf{O}_n)]$.
- Simulate multivariate normal, take max of abs value for each draw, calculate $(\theta_{n,1,j}^+ - \theta_{n,0,j}^+) \pm z_{\max,1-\alpha} \hat{\sigma}_j$.
- Controls FWER.

ABIDE Data

School-age children from Autism Brain Imaging Data Exchange (ABIDEI and ABIDEII) Dataset (Di Martino et al. 2014; 2017)

- in-house preprocessing [fmriprep]
- site harmonization [neuroCombat]
- variables:
 - A : 245 TD ($A=0$), 132 ASD ($A=1$) [377 8-13 yo children].
 - X : age, sex, handedness.
 - Z : autism diagnostic observation schedule, IQ, medication status.
 - M : mean frame-wise displacement (FD).
 - $\Delta=1$: > 5 minutes of data free from ≥ 0.2 framewise displacement (Power et al. 2014) [126 TD (51%), 34 ASD (26%)].
- Y_j : correlation between seed region in DMN and region j , $j = 1, \dots, 400$ (Schafer 400 atlas).
- **SuperLearner** for nuisance regressions: multivariate adaptive regression splines, LASSO, ridge regression, generalized additive models, generalized linear models (with and without interactions, and with and without forward stepwise covariate selection), random forest, and xgboost
- Highly adaptive lasso for conditional density estimation (Hejazi et al. 2022).
- Cross-fitting with 5-fold cross-validation.

ABIDE Inference



Discussion

- We estimate the difference in neural activity between ASD and non-ASD.
- Draw upon idea of a stochastic intervention to estimate brain activity under tolerable motion.
- Incorporate ensemble of machine learning algorithms to flexibly model motion using [SuperLearner](#).
- In ABIDE data analysis, removed motion artifacts while more efficiently using data.
- **Machine-learning based standardization of motion combined with statistical inference.**

Acknowledgment

Thank you!

All authors were supported by the National Institute of Mental Health of the National Institutes of Health under award number R01 MH129855. The content is solely the responsibility of the authors and does not necessarily represent the official views of the National Institutes of Health.

References |

- K. T. Cosgrove, T. J. McDermott, E. J. White, M. W. Mosconi, W. K. Thompson, M. P. Paulus, C. Cardenas-Iniguez, and R. L. Aupperle. Limits to the generalizability of resting-state functional magnetic resonance imaging studies of youth: An examination of abcd study® baseline data. *Brain imaging and behavior*, 16(4):1919–1925, 2022.
- A. Di Martino, C.-G. Yan, Q. Li, E. Denio, F. X. Castellanos, K. Alaerts, J. S. Anderson, M. Assaf, S. Y. Bookheimer, M. Dapretto, et al. The autism brain imaging data exchange: towards a large-scale evaluation of the intrinsic brain architecture in autism. *Molecular psychiatry*, 19(6):659–667, 2014.
- A. Di Martino, D. O'connor, B. Chen, K. Alaerts, J. S. Anderson, M. Assaf, J. H. Balsters, L. Baxter, A. Beggiato, S. Bernaerts, et al. Enhancing studies of the connectome in autism using the autism brain imaging data exchange ii. *Scientific data*, 4(1):1–15, 2017.
- N. S. Hejazi, M. J. van der Laan, and D. C. Benkeser. haldensify: Highly adaptive lasso conditional density estimation in R. *Journal of Open Source Software*, 2022. doi: 10.21105/joss.04522. URL <https://doi.org/10.21105/joss.04522>.
- M. J. Maenner. Prevalence and characteristics of autism spectrum disorder among children aged 8 years—autism and developmental disabilities monitoring network, 11 sites, united states, 2020. *MMWR. Surveillance Summaries*, 72, 2023.
- S. Marek, B. Tervo-Clemmens, F. J. Calabro, D. F. Montez, B. P. Kay, A. S. Hatoum, M. R. Donohue, W. Foran, R. L. Miller, T. J. Hendrickson, S. M. Malone, S. Kandala, E. Feczko, O. Miranda-Dominguez, A. M. Graham, E. A. Earl, A. J. Perrone, M. Cordova, O. Doyle, L. A. Moore, G. M. Conan, J. Uriarte, K. Snider, B. J. Lynch, J. C. Wilgenbusch, T. Pengo, A. Tam, J. Chen, D. J. Newbold, A. Zheng, N. A. Seider, A. N. Van, A. Metoki, R. J. Chauvin, T. O. Laumann, D. J. Greene, S. E. Petersen, H. Garavan, W. K. Thompson, T. E. Nichols, B. T. Yeo, D. M. Barch, B. Luna, D. A. Fair, and N. U. Dosenbach. Reproducible brain-wide association studies require thousands of individuals. *Nature* 2022 603:7902, 603(7902):654–660, 3 2022. ISSN 1476-4687. doi: 10.1038/s41586-022-04492-9. URL <https://www.nature.com/articles/s41586-022-04492-9>.

References II

- A. N. Nielsen, D. J. Greene, C. Gratton, N. U. Dosenbach, S. E. Petersen, and B. L. Schlaggar. Evaluating the prediction of brain maturity from functional connectivity after motion artifact denoising. *Cerebral Cortex*, 29(6):2455–2469, 2019.
- J. D. Power, A. Mitra, T. O. Laumann, A. Z. Snyder, B. L. Schlaggar, and S. E. Petersen. Methods to detect, characterize, and remove motion artifact in resting state fmri. *Neuroimage*, 84:320–341, 2014.
- T. D. Satterthwaite, D. H. Wolf, J. Loughead, K. Ruparel, M. A. Elliott, H. Hakonarson, R. C. Gur, and R. E. Gur. Impact of in-scanner head motion on multiple measures of functional connectivity: relevance for studies of neurodevelopment in youth. *Neuroimage*, 60(1):623–632, 2012.
- B. E. Yerys, E. M. Gordon, D. N. Abrams, T. D. Satterthwaite, R. Weinblatt, K. F. Jankowski, J. Strang, L. Kenworthy, W. D. Gaillard, and C. J. Vaidya. Default mode network segregation and social deficits in autism spectrum disorder: Evidence from non-medicated children. *NeuroImage: Clinical*, 9:223–232, 2015.

Identification

Theorem (Identifiability)

Under the following assumptions:

- (A1) *No missing confounders:* $E_C\{Y(m) | A = a, X, Z\} = E_C\{Y(m) | A = a, M = m, X, Z\}$;
- (A2) *Positivity:*
 - (A2.1) *for every x such that $p_X(x) > 0$, we also have $p_{a|X}(x) > 0$ for $a = 0, 1$;*
 - (A2.2) *for every (x, z, m) such that $p_X(x)p_{Z|a,X}(z | x)p_{M|\Delta=1,0,X}(m | x) > 0$, we also have that $p_{M|a,X,Z}(m | x, z) > 0$ for $a = 0, 1$.*
- (A3) *Causal Consistency: for any child with observed motion value $M = m$, the observed functional connectivity measurement Y is equal to the counterfactual functional connectivity measurement $Y(m)$.*

The counterfactual $\theta_{C,a}$ is identified by θ_a , where

$$\theta_1 = \iiint \mu_{Y|1,M,X,Z}(m, x, z) p_{Z|1,X}(z | x) p_{M|\Delta=1,0,X}(m | x) p_X(x) dz dm dx$$

$$\theta_0 = \iiint \mu_{Y|0,M,X,Z}(m, x, z) p_{Z|0,X}(z | x) p_{M|\Delta=1,0,X}(m | x) p_X(x) dz dm dx$$

Estimation, 1/3

1. *Estimate mean functional connectivity* $\mu_{Y|A,M,X,Z}$. Fit a super learner regression using Y as the outcome and including A , M , X , and Z as predictors. Evaluate the fitted value for $i = 1, \dots, n$ and for $a = 0, 1$.
2. *Estimate motion distributions* $p_{M|A,X}$, $p_{M|\Delta=1,A,X}$, $p_{M|A,X,Z}$, and $p_{M|\Delta=1,A,X,Z}$. Estimate densities using the highly adaptive LASSO and evaluate for $a = 0, 1$ and $i = 1, \dots, n$.
3. *Estimate motion-standardized functional connectivity* $\eta_{\mu|A,Z,X}$. Create the pseudo-outcome $\hat{Y}_{M,i} = \mu_{n,Y|A,M,X,Z}(A_i, M_i, X_i, Z_i) \times \frac{p_{n,M|\Delta=1,A,X}(M_i|0, X_i)}{p_{n,M|\Delta=1,A,X,Z}(M_i|A_i, X_i, Z_i)}$. Using only observations with $\Delta_i = 1$, fit a super learner regression using \hat{Y}_M as the outcome and A , Z , and X as predictors. Set A to a evaluate for $i = 1, \dots, n$.

Estimation, 2/3

4. Estimate Z-standardized functional connectivity $\eta_{\mu|A,M,X}$. Create the pseudo-outcome

$\hat{Y}_{Z,i} = \mu_{n,Y|A,M,X,Z}(A_i, M_i, X_i, Z_i) \times \frac{p_{n,M|A,X}(M_i|A_i, X_i)}{p_{n,M|A,X,Z}(M_i|A_i, X_i, Z_i)}$. Fit a super learner regression using \hat{Y}_Z as the outcome and including M , X , and A as predictors. Set A to a and evaluate for $i = 1, \dots, n$.

5. Estimate motion- and Z-standardized functional connectivity $\xi_{a,\eta|X}$. Fit a super learner regression using $\eta_{n,\mu|A,Z,X}$ as the outcome and including A and X as predictors. For $a = 0, 1$, evaluate the fitted value for $i = 1, \dots, n$.

6. Calculate plug-in estimate. Compute the plug-in estimate $\theta_{n,a} = n^{-1} \sum_{i=1}^n \xi_{n,a,\eta|X}(X_i)$.

Estimation, 3/3

7. Estimate diagnosis distribution π_a and inclusion probability $\pi_{\Delta=1|A,X}$. Fit a super learner regression using A as the outcome and including X as predictors. Evaluate for $i = 1, \dots, n$ and set $\pi_{n,0}(X_i) = 1 - \pi_{n,1}(X_i)$. Then fit a super learner using Δ as the outcome and including A and X as predictors. Set A to 0 to obtain $\pi_{n,\Delta=1|A,X}(0, X_i)$ for $i = 1, \dots, n$. Compute

$$\bar{\pi}_{n,0}(X_i) = \pi_{n,0}(X_i)\pi_{n,\Delta=1|A,X}(0, X_i) \text{ for } i = 1, \dots, n.$$

8. Evaluate estimated efficient influence function $D_{n,a}(O_i)$. For $a = 0, 1$ and each $i = 1, \dots, n$, evaluate $D_{n,a}(O_i)$ by substituting the fitted values based on the estimated nuisance parameters obtained in steps 1-7 into equation (1).

9. Compute the one-step estimator. For $a = 0, 1$, compute $\theta_{n,a}^+ = \theta_{n,a} + n^{-1} \sum_{i=1}^n D_{n,a}(O_i)$.

Simulation: Confirming theoretical properties of estimators

- Simulation Setting

$$X \sim \text{Bin}(1, \frac{1}{2})$$

$$A \sim \text{Bin}(1, \text{expit}(X - \frac{1}{4}))$$

$$Z \sim \text{Bin}(1, \text{expit}(\frac{5}{4}A - \frac{1}{2}))$$

$$M \sim N(1 + A + X/2 - Z/4, 1)$$

$$Y \sim N(-1 + X/2 - Z/3 - A/4 + M/5, 1)$$

sample size $n \in \{200, 500, 1000, 2000, 4000\}$

- evaluate proposed estimators of θ_0 and θ_1

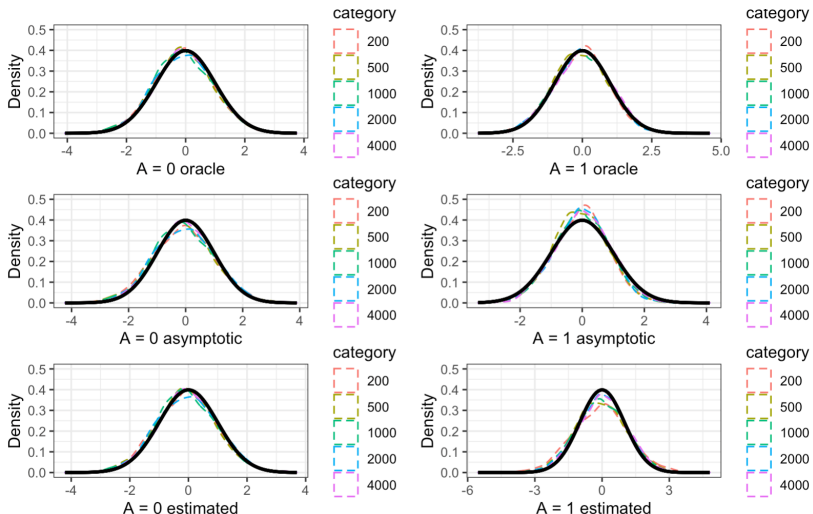
Simulation: Confirming theoretical properties of estimators

Case I: all nuisance parameters are consistently estimated at appropriate rates

n	$\theta_{n,0}^{cf}$				$\theta_{n,1}^{cf}$			
	$n^{1/2}$ bias	$n^{1/2}$ sd	sd ratio	cover	$n^{1/2}$ bias	$n^{1/2}$ sd	sd ratio	cover
200	-0.235	2.063	1.075	0.929	-0.246	2.358	1.430	0.851
500	-0.150	1.938	0.986	0.951	-0.310	2.369	1.205	0.900
1000	-0.141	2.003	1.028	0.940	-0.113	2.333	1.110	0.922
2000	-0.026	1.977	1.033	0.940	-0.077	2.328	1.056	0.931
4000	-0.006	1.913	1.014	0.950	0.076	2.074	0.914	0.979

Table: All nuisance parameters are consistently estimated at appropriate rates with the use of cross-fitting

Simulation: Confirming theoretical properties of estimators



Simulation: Multiple Robustness

Case II: five scenarios in which only certain combinations of nuisance parameters were correctly specified

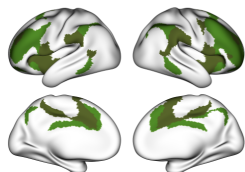
Setting	n	bias _{θ^{gcf}_{n,0}}	sd _{θ^{gcf}_{n,0}}	bias _{θ^{gcf}_{n,1}}	sd _{θ^{gcf}_{n,1}}
$p_{M \Delta=1,0,X}, p_{M a,X,Z}, \pi_a$ correct	200	0.0085	0.1492	0.0915	0.1608
	500	0.0076	0.0890	0.0568	0.0912
	1000	0.0024	0.0627	0.0423	0.0700
	2000	0.0043	0.0440	0.0335	0.0502
	4000	0.0037	0.0309	0.0281	0.0358
$p_{M \Delta=1,0,X}, p_{M a,X,Z}, \xi_{\eta a,X}$ correct	200	-0.0190	0.1458	-0.0318	0.1827
	500	-0.0116	0.0855	-0.0158	0.1030
	1000	-0.0100	0.0600	-0.0082	0.0762
	2000	-0.0040	0.0410	-0.0025	0.0537
	4000	-0.0006	0.0294	0.0022	0.0379
$\pi_a, \bar{\pi}_0, \eta_{\mu a,M,X}, \mu_{Y a,M,X,Z}$ correct	200	-0.0037	0.1472	-0.0137	0.1679
	500	-0.0023	0.0880	-0.0061	0.1012
	1000	-0.0043	0.0616	-0.0026	0.0742
	2000	-0.0007	0.0432	0.0001	0.0527
	4000	0.0009	0.0305	0.0019	0.0372
$\pi_a, p_{M \Delta=1,0,X}, \mu_{Y a,M,X,Z}$ correct	200	-0.0171	0.1512	-0.0273	0.1810
	500	-0.0096	0.0879	-0.0142	0.1019
	1000	-0.0090	0.0621	-0.0074	0.0747
	2000	-0.0032	0.0433	-0.0018	0.0530
	4000	-0.0002	0.0306	0.0019	0.0374
$p_{M \Delta=1,0,X}, \xi_{\eta a,X}, \mu_{Y a,M,X,Z}$ correct	200	-0.0190	0.1458	-0.0318	0.1827
	500	-0.0116	0.0855	-0.0158	0.1030
	1000	-0.0100	0.0600	-0.0082	0.0762
	2000	-0.0040	0.0410	-0.0025	0.0537
	4000	-0.0006	0.0294	0.0022	0.0379

Simulation: Evaluating estimators in the context of ASD

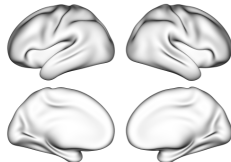
Simulation setting: a data generating process that mimics the real data

- $n = 400$
- First, use real data to estimate functional connectivity between default mode network (seed region) and 6 resting-state networks defined using Yeo 7 parcellation
- A, M, X, Z : similar in distribution to those in the observed data
- $\Delta = 1$ if $M \leq 0.2$
- Y 's follow a multivariate normal distribution
- true associations between 4 regions are set to 0, the remaining 2 regions are assigned non-zero associations

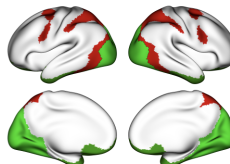
Simulation: Evaluating estimators in the context of ASD

Truth**Significant associations**

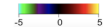
naïve (with participant removal)



naïve (all data)



our method (all data)



Simulation: Evaluating estimators in the context of ASD

True association		Proposed Method	Proposed Method (cross-fitting)	naive with participant removal	naïve
Region 1 0	Bias	0.0045	0.0041	-0.0187	-0.0644
	sd	0.0195	0.0196	0.0191	0.0208
	MSE $\times 10^3$	0.4016	0.4020	0.7145	4.5784
	Type I error	0.0390	0.0150	0.1040	0.8660
Region 2 0	Bias	0.0072	0.0063	0.0177	0.0608
	sd	0.0299	0.0249	0.0240	0.0224
	MSE $\times 10^3$	0.9466	0.6569	0.8902	4.2036
	Type I error	0.0320	0.0110	0.0830	0.7180
Region 3 0	Bias	0.0075	0.0069	0.0156	0.0553
	sd	0.0187	0.0185	0.0180	0.0179
	MSE $\times 10^3$	0.4047	0.3888	0.5680	3.3807
	Type I error	0.0460	0.0170	0.0720	0.8310
Region 4 0	Bias	-0.0036	-0.0034	-0.0178	-0.0662
	sd	0.0192	0.0198	0.0196	0.0204
	MSE $\times 10^3$	0.3824	0.4031	0.7010	4.7970
	Type I error	0.0200	0.0050	0.1080	0.8840
Region 5 -0.0484	Bias	0.0068	0.0042	0.0215	0.0694
	sd	0.0202	0.0212	0.0205	0.0211
	MSE $\times 10^3$	0.4532	0.4673	0.8837	5.2665
	Power	0.4550	0.4100	0.1670	0.1190
Region 6 -0.0682	Bias	0.0056	0.0031	0.0245	0.0798
	sd	0.0163	0.0172	0.0179	0.0214
	MSE $\times 10^3$	0.2976	0.3059	0.9195	6.8226
	Power	0.9380	0.8860	0.5230	0.0630

ABIDE Estimates

